applied sciences

MDPI

*Article*

# Simulation-Based Reliability Design Optimization Method for Industrial Robot Structural Design

**Li-Xiang Zhang [1], Xin-Jia Meng [1,*], Zhi-Jie Ding [1] and Hong-Xiang Han [2]**

[1] School of Mechanical and Equipment Engineering, Hebei University of Engineering, Handan 056038, China
[2] Weihai Zaiyuan Automation Equipment Co., Ltd., Weihai 264200, China
* Correspondence: mxjdoctor@126.com; Tel.: +86-136-7320-1287

**Abstract:** Robots are main elements in Industry 4.0. Research on the design optimization of robots has a great significance in manufacturing industries. There inevitably exist various uncertainties in robot design that have an important influence on the reliability of robots. At present, the design optimization of robots considering the uncertainties is mainly focused on joints design and trajectory optimization. However, for the structural design of robots, deterministic design optimization still plays a leading role. In this paper, a simulation-based reliability design optimization method is proposed to improve the reliability of robots' structural design. In the proposed method, the Latin hypercube sampling (LHS), computer simulation, response surface method (RSM) and SORA (Sequential Optimization and Reliability Assessment) algorithm are integrated to complete the structural design of the robot. Firstly, samples of the uncertainty design variables were obtained by LHS, and then, the reliability performance constraint functions were firstly constructed through the RSM in which the joint simulation of MTLAB and ANSYS was adopted. Afterwards, the reliability design optimization model was established on the basis of the probabilistic reliability theory. At last, the SORA algorithm was employed to realize the optimization. The design optimization problems of the big arm and the small arm of a 6 Kg industrial robot were considered to verify the proposed method. The results showed that the weights of the big arm and the small arm were, respectively, reduced by 7.73% and 25.70% compared with those of the original design, and the design was more effective in ensuring the reliability requirements compared with the deterministic optimization. Moreover, the results also demonstrated that the proposed method has a better computational efficiency compared with the reliability design optimization of the double-loop method.

**Keywords:** industrial robot; reliability design optimization; big arm; small arm; computer simulation

check for updates

**Citation:** Zhang, L.-X.; Meng, X.-J.; Ding, Z.-J.; Han, H.-X. Simulation-Based Reliability Design Optimization Method for Industrial Robot Structural Design. *Appl. Sci.* **2023**, *13*, 3776. https://doi.org/10.3390/app13063776

Academic Editors: Luigi Fortuna, Yutaka Ishibashi and Marco Troncossi

Received: 30 January 2023
Revised: 9 March 2023
Accepted: 14 March 2023
Published: 15 March 2023

**Copyright:** © 2023 by the authors. Licensee MDPI, Basel, Switzerland. This article is an open access article distributed under the terms and conditions of the Creative Commons Attribution (CC BY) license (https://creativecommons.org/licenses/by/4.0/).

## 1. Introduction

Since flexible manufacturing systems rapidly developed in recent years, industrial robots play a more and more important role in various manufacturing scenarios [1]. The modern application of industrial robots includes welding, assembly, painting, machining and so on. The continually expanding application of industrial robots brings new challenges, which include higher performance demands, such as faster responses, less energy consumption and greater robustness. The robot body design has a direct effect on its performance, and an excellent robot body design is generally regarded as a significant foundation for good performance [2]. Therefore, the development of efficient industrial robot design methods has increasingly attracted wide attention. Either design optimization technology or simulation-based design technology can effectively support the design and development of industrial robots. In addition, the simulation technology and robot design optimization technology, as the main components of Industry 4.0 [3–5], have a very important significance in the development of manufacturing industries.

The design optimization technology as an important measure has been broadly employed to improve the design and reduce the costs in many product designs, such as car

design, airplane design, ship design, etc. Due to its outstanding advantages, more and more design optimization methods have been developed for robot body design. Hsiao et al. [6] proposed a surrogate-based evolutionary optimization method, in which the response surface method is integrated with a multi-objective evolutionary algorithm. Their proposed method can not only improve the robot arm performance, but also alleviate the computational burden. Kouritem et al. [7] proposed a multi-objective design mechanism for industrial robots. In this design mechanism, the initial and running costs, the stress analysis and the vibration analysis are considered, and therefore the optimum type of material and physical dimensions can be selected for industrial robot arms. Liang et al. [8] proposed a structural optimization method for robot arms, which specially considers the influences of flexible joints on robot dynamics. Bugday and Karali [9] analyzed different robot arms designs, in which both geometry and materials are changed, and their findings showed that the cost, efficiency and motor lifetime were all improved by adopting the optimization technology.

In addition to the optimization design, the simulation design is an advanced technology that is often used in modern product design. The simulation-based design is practically used to predict the behavior and results of products [10]. Benefited from the development of computer technology, computer simulation design has been widely used in modern mechanical product design, greatly improving design efficiency and product quality. Similar to most mechanical product designs, industrial robot design also extensively adopts computer simulation methods. Ramasubramanian et al. [11] used a commercial CAD platform to perform the initial design of a robot gripper finger. Brathikan et al. [12] employed the dynamics simulation software ADAMS to analyze the kinematics of a five-axis industrial robotic arm. Sahu et al. [13,14] optimized the performance of a six-axis industrial robot on the basis of stress, modal, and vibration analyses by using FEM of the ANSYS workbench. Ghosh et al. [15] modified the design of the robotic arm based on the analysis of von Mises stress and strain by using ANSYS simulation. Shanmugasundar et al. [16] proposed an optimization framework to carry out a structural optimization design of a five-DOF welding robot considering the strength, stiffness, and robot weight by using ANSYS.

The above-mentioned research on the structural optimization and simulation design of robots was completed with a deterministic analysis. However, there inevitably exist various uncertainties in actual engineering [17], for example, the variation of the coefficient related to a material's properties derived from the discreteness of engineering material properties [18], the variation of the dimensions related to manufacturing errors [19], etc. The deterministic design ignores the influence of uncertainties, which generally yields unreliable design results, especially in the optimization design. In the design of an industrial robot, uncertainties are also an important factor to be considered. **Xu** et al. [20] proposed a dynamic and static structural topology optimization method with uncertain parameters for the lift arm of a parking robot. Wang et al. [21] performed a trajectory optimization under non-probabilistic time-dependent reliability constraints to improve the soaring operating performance of robotic manipulators. Gao et al. [22] realized the design optimization of clearance joints based on reliability sensitivity analysis. Lara-Molina et al. [23] constructed the dynamic modeling of a one-link flexible manipulator using the stochastic finite element method in terms of the displacement of the manipulator's tip and the frequency response function subjected to uncertainties. Lara-Molina et al. [24] also proposed a novel robust optimal design for parallel manipulators to optimize the performance indices subject to the unavoidable effect of the uncertainties. Currently, the design optimization of a robot considering the uncertainties is mainly focused on the joints design and the trajectory optimization. As for the structural design of a robot, it is mainly performed by the deterministic design optimization.

Through the above analysis, the reliability design optimization for a robot is very important for improving the reliability of an industrial robot structural design. Moreover, improving the calculation efficiency of the method can effectively promote the application of the method in engineering. Therefore, in this paper, a simulation-based reliability design

optimization method (SBRDOM) is prosed for an industrial robot structural design. In the proposed method, the simulation design is integrated with the reliability design optimization to obtain a robot structural design model, and therefore, the best balance between economy and safety could be achieved during the robot structural design. Furthermore, the SORA algorithm was employed to solve the problem of low computational efficiency of reliability design optimization in engineering applications.

The remainder of this paper is organized as follows. Section 2 provides the proposed SBRDOM, including the SBRDOM procedure, the formulation of the reliability design optimization model and the SORA algorithm and its associated mathematical formulation. In Section 3, the design of the big arm and small arm is used to demonstrate the validity of the proposed method. Finally, Section 4 concludes this work and suggests future work.

## 2. Simulation-Based Reliability Design Optimization Method (SBRDOM)

### 2.1. SBRDOM Procedure

In the SBRDOM, the Latin hypercube sampling (LHS), simulation technology, response surface method (RSM) and SORA (Sequential Optimization and Reliability Assessment) algorithm were integrated to complete the structural design of the robot. The proposed method integrated the joint simulation of MTLAB and ANSYS into approximate technology so as to obtain the performance function of an industrial robot. In addition, the proposed method employed the SORA algorithm to solve the problem of low computational efficiency in engineering applications. The main procedure of the SBRDOM is shown in Figure 1.

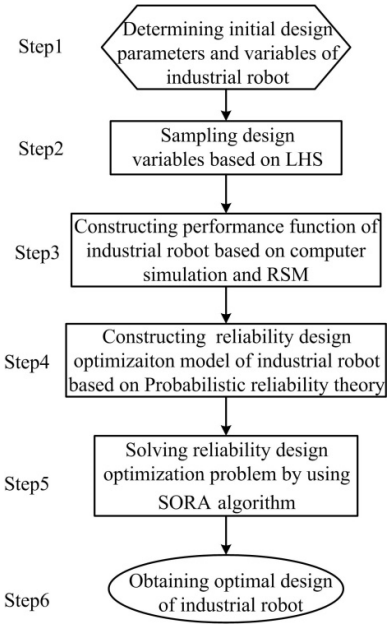



**Figure 1.** Main procedure of the SBRDOM.

The main steps of the proposed method are summarized as follows.

Step 1: Determining the initial design parameters and variables of the industrial robot. In this step, the geometric configuration, load, material and working environment of the industrial robot were analyzed to define the uncertainty design parameters and variables.

Step 2: Sampling the design variables based on LHS. In this step, the LHS [25] was used to obtain the samples of the design variables. The bounds of each variable were regarded as an interval. This interval was divided into $n$ small intervals, and then a sample point was randomly extracted from each small interval. The final samples were obtained by combining all the sample points.

Step 3: Constructing the performance function of the industrial robot based on computer simulation and RSM. In this step, the joint simulation of MTLAB and ANSYS was

integrated with RSM to obtain the preformance function of the industrial robot. The detailed operation of this step is shown in Figure 2 and explained as follows,

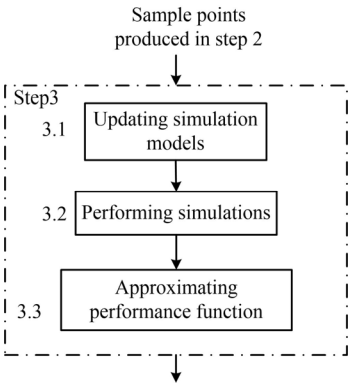



**Figure 2.** Detailed operation of step 3.

Step 3.1: Updating the simulation models. Firstly, the 3D parameter model of the industrial robot was constructed by using the ANSYS software. Then, the computer simulation model was updated with the sample point produced in step 2.

Step 3.2: Performing the simulations. The ANSYS simulation was performed with each sample, and then the response values corresponding to each sample were obtained.

Step 3.3: Approximating the performance function by using RSM. In this step, MATLAB was used to apply the approximation technology. Based on the samples and responses, the performance function could be obtained by using the approximation approach. The general used approximate model included a polynomial model, a kriging model and a support vector machine model.

Step 4: Constructing the reliability design optimization model of the industrial robot based on the probabilistic reliability theory. Based on the probability reliability theory [26], the design parameters and variables were modeled as random parameters and variables, and then the reliability design optimization model of the industrial robot could be constructed.

Step 5: Solving the reliability design optimization problem by using the SORA algorithm. The reliability design optimization model of the industrial robot was carried out by employing the SORA algorithm in this step. The process of SORA is detailed in Section 2.3.

Step 6: Obtaining the optimal design of the industrial robot. In this step, the optimization results obtained by SORA were evaluated. If the results were not reasonable, we turned back to Step 2 to perform the process again. The evaluation criterion was that the difference between two optimization results had to be within the allowable accuracy range.

### *2.2. Formulation of the Reliability Design Optimization Model*

The general reliability design optimization model for the industrial robot is presented as follows:

$$\begin{aligned} &\min\ f(\boldsymbol{\mu}_{\mathbf{x}}) \\ &\text{s.t. } \Pr[g_i(\mathbf{x}_r, \mathbf{p}_r) < 0] \geq R_t \\ &\quad \boldsymbol{\mu}_{\mathbf{x}}^L \leq \boldsymbol{\mu}_{\mathbf{x}} \leq \boldsymbol{\mu}_{\mathbf{x}}^U \\ &\quad i = 1, 2, \cdots, n \end{aligned} \tag{1}$$

where $f$ is the objective function, $\mathbf{x}_r$ is the vector of the random design variable, $\boldsymbol{\mu}_{\mathbf{x}}$ is the vector of the mean values of the random design variable, $\mathbf{p}_r$ is the vector of the random design parameter, Pr stands for the probability, $g_i$ is the $i$th performance constraint function, $n$ is the number of the performance constraint function, and the superscripts $L$ and $U$, respectively, stand for upper boundary and lower boundary.

The performance constraint function was obtained by using the approximate model, and therefore $g_i$ was an implicit function. The expression of $g_i$ depends on the selection of the approximate model. Since different approximate models have different accuracy and efficiency, the approximate model to be selected relies on the specific context. In this

proposed method, the quadratic polynomial with cross terms was chosen for fitting the performance constraint function, which is given below.

$$\hat{g}(\mathbf{x}) = a_0 + \sum_{i=1}^{m} b_i x_i + \sum_{i=1}^{m} c_i x_i^2 + \sum_{i=1}^{m} \sum_{j=i+1}^{m} d_{ij} x_i x_j \tag{2}$$

where $\hat{g}(\mathbf{x})$ stands for the approximation of the performance constraint function, $a_0$, $b_i$, $c_i$ and $d_{ij}$ are coefficients, $x_i$ and $x_j$ is the $i$th or the $j$th random design variable, $m$ is the number of the random design variable.

### *2.3. SORA and Its Associated Mathematical Formulation*

It has been practically testified that SORA [27] is an efficient algorithm to solve reliability design optimization problems, which has been widely used due to its high efficiency. In SORA, the optimization solution process is decomposed into a deterministic optimization and an uncertainty analysis, which are executed alternately. The detailed process of SORA is shown in Figure 3 and explained as follows.

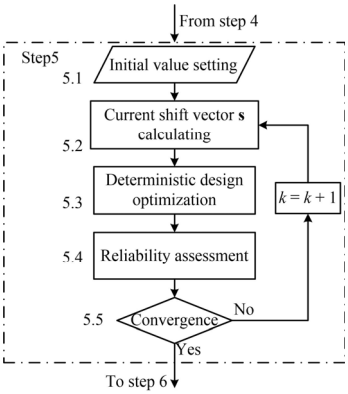



**Figure 3.** Detailed process of SORA.

Step 5.1: Initial value setting. The starting points including the design variables and the parameters were set. Let the shift vector s = 0, and set the iteration number $k$ = 1. Set $\mathbf{p}_{\mathbf{iMPP}} = \boldsymbol{\mu}_{\mathbf{p}}^{(0)}$, $\mathbf{x}_{\mathbf{iMPP}}^{(0)} = \boldsymbol{\mu}_{\mathbf{x}}^{(0)}$, where the superscript (0) stands for the initial iteration, and $\mathbf{p}_{\mathbf{iMPP}}$ and $\mathbf{x}_{\mathbf{iMPP}}$ stand for the inverse most probable point (iMPP) of the random parameter and the iMPP of the random variable, respectively.

Step 5.2: Current shift vector **s** calculation. The shift vector **s** is calculated by

$$\mathbf{s}_i = \boldsymbol{\mu}_{\mathbf{x}}^{(k)} - \mathbf{x}_{\mathbf{iMPP}}^{(k)} \tag{3}$$

where $\mathbf{s}_i$ is the vector of the shift vector corresponding to the $i$th performance constraint function, $k$ stands for the $k$th iteration, $\mathbf{x}_{\mathbf{iMPP}}^{(k)}$ is the iMPP corresponding to the $i$th performance constraint function.

Step 5.3: Deterministic design optimization. In this step, the deterministic design optimization was conducted, whose model is given as follows.

$$\begin{aligned} &\min\ f(\boldsymbol{\mu}_{\mathbf{x}}) \\ &\text{s.t. } g_i(\boldsymbol{\mu}_{\mathbf{x}} - \mathbf{s}_i, \mathbf{p}_{\text{iMPP}}) < 0 \\ &\quad \boldsymbol{\mu}_{\mathbf{x}}^{L} \le \boldsymbol{\mu}_{\mathbf{x}} \le \boldsymbol{\mu}_{\mathbf{x}}^{U} \\ &\quad i = 1, 2, \cdots, n \end{aligned} \tag{4}$$

Step 5.4: Reliability assessment. $\mathbf{p_{iMPP}}$ and $\mathbf{x_{iMPP}}$ could be determined by using the reliability assessment, which was conducted through the following optimization model.

$$\begin{aligned} &\max \quad G_i(\mathbf{u}) \\ &s.t. \quad \|\mathbf{u}\| = \Phi^{-1}(R_t) \end{aligned} \tag{5}$$

where $G_i$ is the $i$th performance function in standard normal space (u-space), and $\mathbf{u}$ is the vector of standard normal random variables and parameters, that is $\mathbf{u} = [\mathbf{u_p}, \mathbf{u_x}]$. $\mathbf{u_p}$ and $\mathbf{u_x}$ are transformed from the original vector of random variables and random parameters, respectively. For the transformation formulas, please refer to Ref. [28].

Step 5.5: Convergence judgment. Judging whether the objective function achieved convergence and whether the constraints were respected. If the convergence criterion os met, then go to step 6, otherwise let $k = k + 1$ and proceed to the next iteration.

## 3. Demonstrative Example

### *3.1. Simulation Model of a Mechanical Arm*

The ANSYS software was used to perform a static structural analysis. Taking an industrial robot with a load weight of 6 Kg as the object, the reliability design optimization of its big arm and small arm was carried out by using the proposed method. The structure of the mechanical arms is shown in Figure 4.

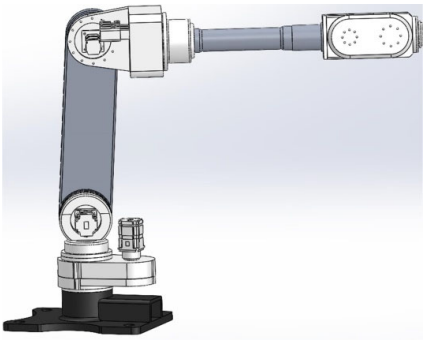


**Figure 4.** Structure of the mechanical arms.

When the finite element analysis model was established, the body mesh method was employed in order to measure more precise values during the mesh analysis. The three-node triangular element was chosen as the element type, and the element size was set to 2 mm. For the big arm, the number of nodes was 108,657 and the number of element was 58,479, while for the small arm, the number of node was 87,781 and the number of element was 50,160. The mesh analysis of the big arm and the small arm is shown in Figures 5 and 6.

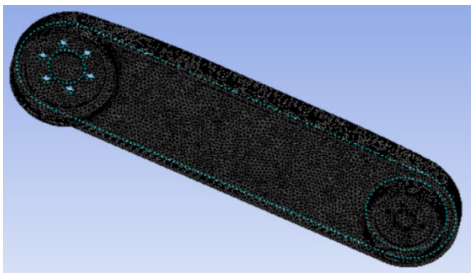


**Figure 5.** Finite element analysis model of the big arm.

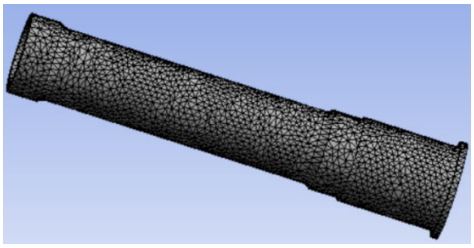


**Figure 6.** Finite element analysis model of the small arm.

The limit state (that is, the horizontal position) was considered to finish the simulation analysis, and the force analysis of the mechanical arm is shown in Figure 7. In Figure 7, $G_{arm1}$ and $G_{arm2}$ represent the gravity of the big arm and the small arm, respectively. $G_{drive}$ and $G_{wrist}$ represent the motor gravity and wrist gravity of the big arm and the small arm, respectively. $F_{max}$ is the maximum load that the robot arm can lift. According to the force analysis and to Ref. [9], the loads and constraints of the mechanical arms could be applied as shown in Figure 8. In Figures 7 and 8, A, B and C represent the joins of the robotic arms, and the details are as follows: A represents joint of first and second links, B represents joint of second and third links, C represents joint of third and fourth links.

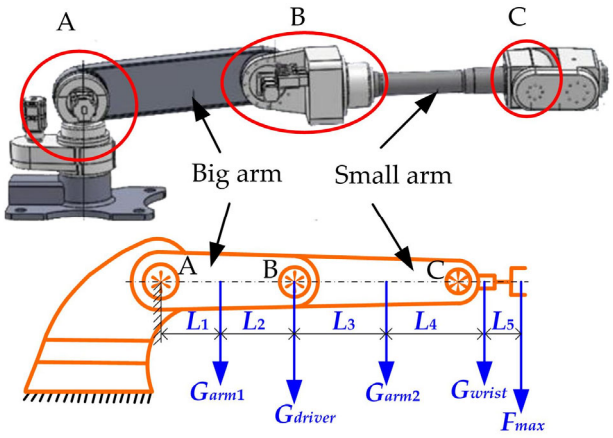



**Figure 7.** Force analysis.

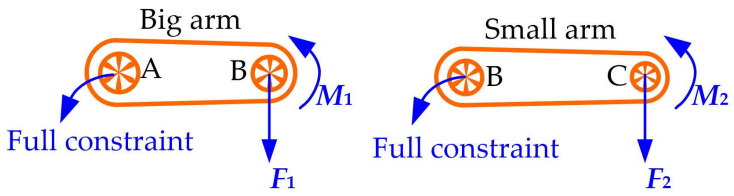



**Figure 8.** Application of loads and constraints.

For the big arm, the full constraints were applied to the end A, while the force $F_1$ and the moment $M_1$ were applied to the end B. For the small arm, the full constraints were applied to the end B, while the force $F_2$ and the moment $M_2$ were applied to the end C. The force and the moment can be calculated by

$$\begin{aligned} F_1 &= G_{arm2} + G_{wrist} + F_{\max} \\ M_1 &= G_{arm2}L_3 + G_{wrist}(L_3 + L_4) + F_{\max}(L_3 + L_4 + L_5) \\ F_2 &= G_{wrist} + F_{\max} \\ M_2 &= G_{wrist}(L_3 + L_4) + F_{\max}(L_3 + L_4 + L_5) \end{aligned} \tag{6}$$

The material properties and loads are listed in Table 1, and the stress and deformation distribution on the big arm and the small arm are shown in Figures 9 and 10.

**Table 1.** Material properties and loads.

| Parameter | Value |
|---|---|
| Elastic modulus | 72 GPa |
| Poisson's ratio | 0.33 |
| Density | 2770 kg/m$^3$ |
| Force $F_1$ | 469.71 N |
| Moment $M_1$ | 130.96 N·m |
| Force $F_2$ | 118.75 N |
| Moment $M_2$ | 58.8 N·m |

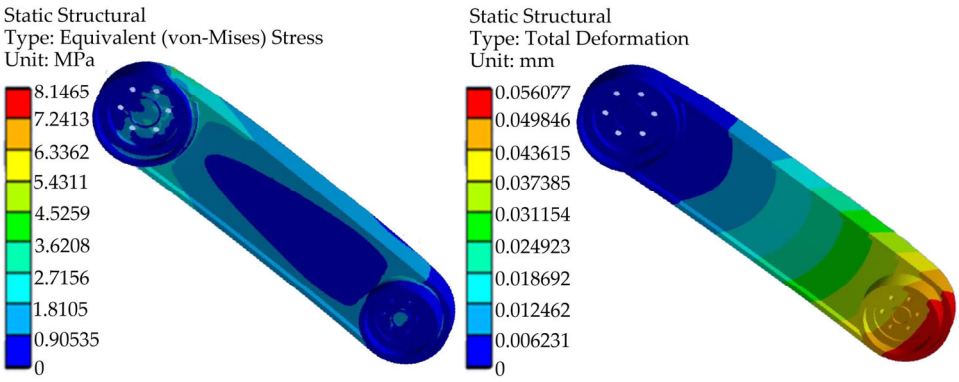



**Figure 9.** Stress and deformation distribution for the big arm.

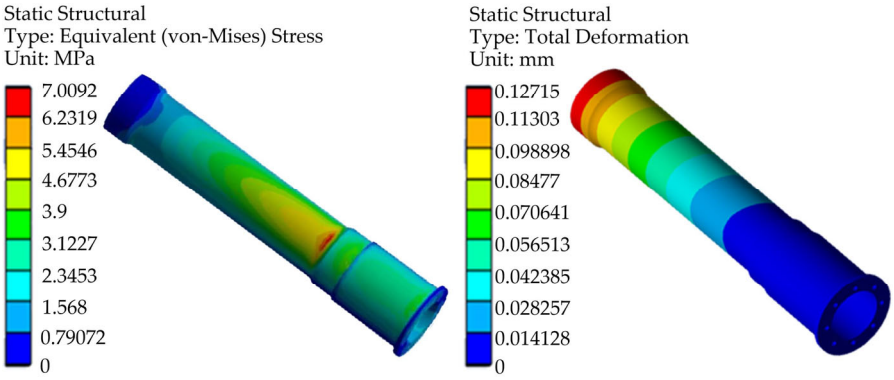



**Figure 10.** Stress and deformation distribution for the small arm.

It can be seen in Figures 8 and 9 that, in the current design, the maximum stress on the big arm was 8.1465 MPa, and the maximum deformation was 0.056077 mm, whereas the maximum stress on the small arm was 7.0092 MPa, and the maximum deformation was 0.12715 mm.

The 3D parameter simulation models of the big arm and the small arm above-mentioned were established by the parameter design language of ANSYS (APDL). The APDL command of the full simulation process contains geometric modeling, mesh generation, material property settings, load and constraint imposition and simulation solution settings. The APDL command was used to complete the simulation of the different samples in order to obtain the performance function of the reliability design optimization model.

### *3.2. Uncertainty Modelling*

The impact of uncertainties was considered in the design optimization of the robot. When the reliability design optimization of the big arm and small arm was performed, three structure variables were considered as the uncertainty design variables, and two performance parameters were considered as the uncertainty design parameters for the big and small arm, respectively. The distribution of the uncertainties is shown in Table 2.

**Table 2.** Distribution of the uncertainties.

| Uncertainty | Distribution | Mean | | Standard |
|---|---|---|---|---|
| | | Low | Up | |
| $x_1$ | Normal | 2 mm | 12 mm | $0.1\mu_{x_1}$ |
| $x_2$ | Normal | 3 mm | 15 mm | $0.1\mu_{x_2}$ |
| $x_3$ | Normal | 2 mm | 12 mm | $0.1\mu_{x_3}$ |
| $x_4$ | Normal | 6 mm | 18 mm | $0.1\mu_{x_4}$ |
| $x_5$ | Normal | 2 mm | 15 mm | $0.1\mu_{x_5}$ |
| $x_6$ | Normal | 8 mm | 20 mm | $0.1\mu_{x_6}$ |
| $\sigma_s$ | Normal | 210 MPa | 210 MPa | 18 MPa |
| $\varepsilon_1$ | Normal | 0.08 mm | 0.08 mm | 0.008 mm |
| $\varepsilon_2$ | Normal | 0.1 mm | 0.1 mm | 0.01 mm |

The symbols $x_1$, $x_2$ and $x_3$ are the geometrical structure parameters of the big arm shown in Figure 11, while the symbols $x_4$, $x_5$ and $x_6$ are the geometrical structure parameters of the small arm shown in Figure 12. $x_1$, $x_2$, $x_3$, $x_4$, $x_5$ and $x_6$ are all random variables of a normal distribution with mean value ($\mu_{x_i}$, $i$ = 1,2, . . . ,6) and standard deviation (0.1 $\mu_{x_i}$, $i$ = 1,2, . . . ,6). $\sigma_s$ is the yield strength, $\varepsilon_1$ and $\varepsilon_2$ are the allowable maximum deformation of the big arm and the small arm, respectively, $\sigma_s$, $\varepsilon_1$ and $\varepsilon_2$ are three random parameters rather than random variables, which all obey a normal distribution.

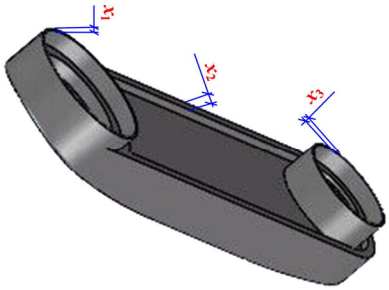



**Figure 11.** Geometrical structure of the big arm.

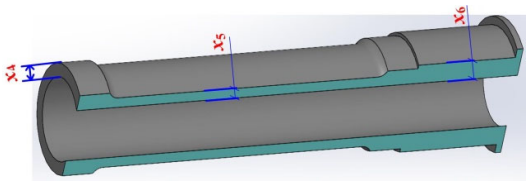



**Figure 12.** Geometrical structure of the small arm.

### *3.3. Reliability Design Optimization Model*

In the structure optimization design of the big arm and the small arm, the impact of uncertainties was considered. With the lightest weight of the robotic arm as the goal, the yield stress and deformation meeting the allowable requirements as the performance constraints, an initial model of the reliability design optimization of the manipulator was constructed. The initial reliability design optimization model of the big arm was:

$$\begin{aligned} \min \quad & f(\mu_{x_1}, \mu_{x_2}, \mu_{x_3}) \\ & = 4.16(70 + \mu_{x_1})^2 \times 10^{-4} + 0.02\mu_{x_2} \\ & -2.1(72.5 - 2\mu_{x_2})^2 \times 10^{-4} \\ & +0.83 \times (105 + 2\mu_{x_3})^2 \times 10^{-4} + 6.69 \\ s.t. \quad & C_1 = \text{Prob}[(\sigma_s - \hat{g}_1(x_1, x_2, x_3)) > 0] \geq 0.9987 \\ & C_2 = \text{Prob}[(\varepsilon_1 - \hat{g}_2(x_1, x_2, x_3)) > 0] \geq 0.9987 \\ & 2 \leq \mu_{x_1} \leq 12 \quad 3 \leq \mu_{x_2} \leq 15 \quad 2 \leq \mu_{x_3} \leq 12 \end{aligned} \tag{7}$$

The initial model for the reliability design optimization of the boom was:

$$\begin{aligned} \min f(\mu_{x_4}, \mu_{x_5}, \mu_{x_6}) &= 4.06 \times 10^{-2} + 4.16\mu_{x_4}^2 \times 10^{-4} \\ &\quad +2.08\mu_{x_4} \times 10^{-2} + 1.91\mu_{x_5}^2 \times 10^{-3} \\ &\quad +9.57\mu_{x_5} \times 10^{-2} + 6.66\mu_{x_6}^2 \times 10^{-4} \\ &\quad +3.33\mu_{x_6} \times 10^{-2} \\ s.t.\ \ C_3 &= \text{Prob}[(\sigma_s - \hat{g}_3(x_4, x_5, x_6)) > 0] \geq 0.9987 \\ C_4 &= \text{Prob}[(\varepsilon_2 - \hat{g}_4(x_4, x_5, x_6)) > 0] \geq 0.9987 \\ C_5 &= \mu_{x_4} - \mu_{x_5} \geq 1.5; C_6 = \mu_{x_6} - \mu_{x_4} \geq 1.5 \\ 6 \leq \mu_{x_4} &\leq 18,\ 2 \leq \mu_{x_5} \leq 15,\ 8 \leq \mu_{x_6} \leq 20 \end{aligned} \tag{8}$$

In Equations (7) and (8), $C_1$ and $C_2$ are the constraints of the strength reliability and stiffness reliability of the big arm, $C_3$ and $C_4$ are the constraints of the strength reliability and stiffness reliability of the small arm, $C_5$ and $C_6$ are the geometric structure constraints of the small arm. The strength reliability and the stiffness reliability were modeled by the stress and the deformation of the robot arms, respectively. The minimum allowable reliability was $R_t = 0.9987$. The function $\hat{g}_i (i = 1, 2, 3, 4)$ of the reliability constraints is the implicit function. Through adding the reliability constraints in the design optimization, a lightweight design of the robot could be obtained under the condition of meeting certain reliability performance requirements. It is noted that the models of Equations (7) and (8) only consider the reliability requirements under static performance and do not consider the reliability requirements under dynamic performance. Additionally, the establishment of the model also did not consider the influence of the jump resonance. However, the jump resonance will inevitably occur due to the decay of the device mechanical properties [29]. This will also affect the reliability of the robotic arm.

The function could be obtained by the step 2 and step 3 of the proposed method, and Equation (2) was adopted as the approximation function. The ANSYS v. 18.1 and MATLAB v. R2021b software were combined to complete this process. The data transfer from MATLAB and ANSYS was performed as follows: (1) MATLAB was used to obtain the samples of the uncertainties, and then we used the "save" function to save the samples data as a "txt" file readable by ANSYS; (2) ANSYS was activated by the "system" statement of MATLAB; (3) ANSYS used the APDL command "VREAD" to read the "txt" file of the samples data saved by MATLAB; (4) ANSYS invoked the APDL command established by Section 3.1 to carry out the simulation for all the samples, and the results of maximum stress and deformation were also saved as a "txt" file using the APDL command "MWRITE": (5) MATLAB read the results file by the "load" function, and then the coefficient of the approximation function was obtained by data fitting of MATLAB. The coefficients of the approximation function are reported in Table 3.

**Table 3.** Coefficients of the approximation function.

| Coefficient | Big Arm | | Small Arm | |
|---|---|---|---|---|
| | Stress $\hat{g}_1(x_1,x_2,x_3)$ | Deformation $\hat{g}_2(x_1,x_2,x_3)$ | Stress $\hat{g}_3(x_4,x_5,x_6)$ | Deformation $\hat{g}_4(x_4,x_5,x_6)$ |
| $a_0$ | 16.08 | 0.09 | 76.08 | 1.04 |
| $b_1$ | −0.79 | $4.2 \times 10^{-3}$ | 0.3 | $2.92 \times 10^{-3}$ |
| $b_2$ | −0.87 | $3.63 \times 10^{-3}$ | −8.5 | −0.12 |
| $b_3$ | −0.04 | $2.85 \times 10^{-4}$ | −2.4 | −0.04 |
| $c_1$ | $4.43 \times 10^{-5}$ | $1.05 \times 10^{-4}$ | $-4.6 \times 10^{-3}$ | $-1.84 \times 10^{-5}$ |
| $c_2$ | 0.03 | $9.89 \times 10^{-5}$ | 0.33 | $4.89 \times 10^{-3}$ |
| $c_3$ | $5.9 \times 10^{-3}$ | $-8.72 \times 10^{-6}$ | 0.09 | $1.36 \times 10^{-3}$ |
| $d_{12}$ | 0.027 | $5.28 \times 10^{-5}$ | $-5.8 \times 10^{-3}$ | $-7.65 \times 10^{-5}$ |
| $d_{13}$ | 0.013 | $-2.7 \times 10^{-6}$ | −0.02 | $-1.9 \times 10^{-4}$ |
| $d_{23}$ | −0.01 | $-7.37 \times 10^{-6}$ | 0.017 | $1.84 \times 10^{-4}$ |

### *3.4. Optimization Result Analysis*

The reliability design optimization model by Equations (7) and (8) was solved by the SORA method. The results for the big arm and the small arm are shown in Tables 4 and 5, respectively.

**Table 4.** Reliability design optimization results for the big arm.

| Item | Original Design | Deterministic Optimization | Proposed Reliability Optimization |
|---|---|---|---|
| ($x_1$, $x_2$, $x_3$) | (11, 9.5, 8) mm | (2, 3, 2) mm | (8.79, 3.54, 2) mm |
| Weight | 10.22 Kg | 8.96 Kg | 9.43 Kg |
| Strength reliability | 1 | 1 | 1 |
| Stiffness reliability | 0.9999989 | 0.63407 | 0.99884 |

**Table 5.** Reliability design optimization results for the small arm.

| Item | Original Design | Deterministic Optimization | Proposed Reliability Optimization |
|---|---|---|---|
| ($x_4$, $x_5$, $x_6$) | (16.5, 13, 18) mm | (9.8, 8.3, 11.3) mm | (12.08, 10.58, 13.58) mm |
| Weight | 2.84 Kg | 1.67 Kg | 2.11 Kg |
| Strength reliability | 1 | 1 | 1 |
| Stiffness reliability | 0.99926 | 0.5 | 0.99872 |

In order to better analyze the design results by different design methods, the results by the deterministic optimization and original design are also shown in Tables 4 and 5. It can be seen in Tables 4 and 5 that the weight and the stiffness reliability by the proposed reliability design optimization were between those obtained with the deterministic design optimization and the original design. All three designs had the same strength reliability. Compared with the deterministic design optimization, the results of the proposed method had a higher weight (the big arm weighed 9.43 Kg, and the small arm 2.11 Kg, while the weights by deterministic design optimization were 8.96 Kg and 1.67 Kg, respectively). However, the stiffness reliability of the deterministic design optimization (for the big arm, it was only 0.63407, and for the small arm, it was 0.5) was much lower than that of the proposed method (for the big arm, it was 0.9999989, and for the small arm, it was 0.99926). This shows that although the deterministic optimization could obtain the lightest weight, its design results could not satisfy the design requirements of the stiffness reliability. This indicates that the design of the proposed method is more reliable than that of the deterministic optimization. For the original design, both the weight and the reliability were the highest. Compared with the original design, the proposed method could reduce the weights of the big arm and the small arm by 7.73% and 25.70%, respectively, and meanwhile satisfy the 0.9987 reliability requirements. This indicates that the design optimization of the proposed method can reduce the weight as much as possible while satisfying the reliability design requirements. All the above descriptions demonstrate that the method proposed in this paper can effectively complete the structural reliability design optimization of industrial robots.

Modal analysis is an important means to understand the vibration of a designed industrial robot; therefore, a modal analysis of the big arm and the small arm was performed. The ANSYS results under the first-order modality are shown in Figures 13 and 14. The frequencies under the original design and the reliability optimization design for the different modality shapes are presented in Table 6.

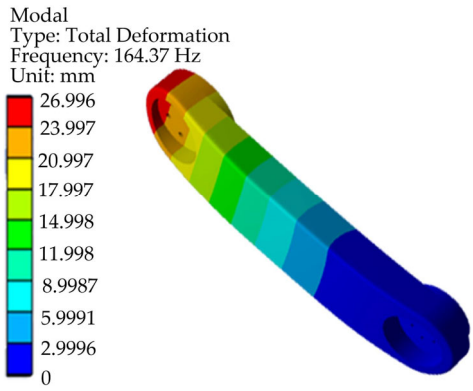



**Figure 13.** Total deformation of the big arm under the first-order modality.

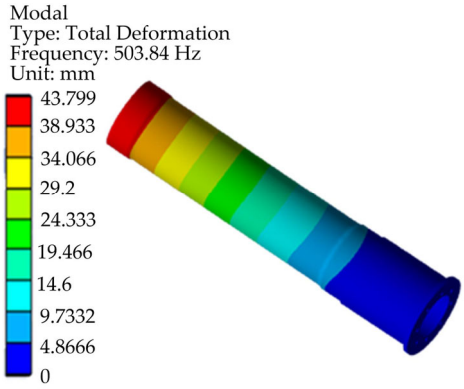



**Figure 14.** Total deformation of the small arm under the first-order modality.

**Table 6.** Frequencies for the different modality shapes.

| Mode | Big Arm | | Small Arm | |
|---|---|---|---|---|
| | Original Design | Reliability Optimization Design | Original Design | Reliability Optimization Design |
| 1 | 150.48 Hz | 164.37 Hz | 490.15 Hz | 503.84 Hz |
| 2 | 448.76 Hz | 465.17 Hz | 490.17 Hz | 503.85 Hz |
| 3 | 745.96 Hz | 840.06 Hz | 2314.6 Hz | 2295.7 Hz |
| 4 | 813.27 Hz | 866.96 Hz | 2331.6 Hz | 2391.4 Hz |
| 5 | 1921.7 Hz | 1939.4 Hz | 2331.7 Hz | 2391.5 Hz |
| 6 | 2003.7 Hz | 2048.3 Hz | 3727.6 Hz | 3696.8 Hz |

The modal analysis results showed that the frequencies of the big arm and the small arm under the first-order modality in the design of the reliability optimization were 164.37 Hz and 503.84 Hz, respectively. In Table 6, the first six natural frequencies of the big arm range from 164.37 Hz to 2048.3 Hz for the reliability optimization design and from 150.48 Hz to 2003.7 Hz for the original design. In additional, the first six natural frequencies of the small arm range from 503.84 Hz to 3696.8 Hz for the reliability optimization design and from 490.15 Hz to 3727.6 Hz for the original design. For neither the big arm nor the small arm, the minimum natural frequency under the reliability optimization design was greater than that under the original design. The results of the modal analysis indicated that the design result of the reliability optimization was more reasonable.

In addition, the reliability design optimization model according to Equations (7) and (8) was also obtained by the double-loop procedure [27] of the reliability design optimization in order to verify the effectiveness of the proposed method. The comparison results are shown in Table 7.

**Table 7.** Comparison of different reliability design optimization methods.

| Method | Big Arm | | Small Arm | |
|---|---|---|---|---|
| | [($x_1$, $x_2$, $x_3$), Weight] | Time | [($x_4$, $x_5$, $x_6$), Weight] | Time |
| Proposed SBRDOM | [(8.79, 3.54, 2) mm, 9.4306 Kg] | 2097.35 s | [(12.08, 10.58, 13.58) mm, 2.1133 Kg] | 1857.24 s |
| double-loop method | [(8.75, 3.56, 2) mm, 9.4295 Kg] | 5853.61 s | [(12.06, 10.52, 13.61) mm, 2.1061 Kg] | 4558.22 s |

In Table 7, the RBDO results obtained with the proposed SBRDOM are close to those obtained by the RBDO method based on the double-loop procedure. However, the simulation time of the proposed SBRDOM is much shorter than that of the RBDO method based on the double-loop procedure. This demonstrated that the proposed method can improve the computational efficiency while ensuring the reliability of the optimization results.

## 4. Conclusions

Considering that the influence of uncertainties in the structural design of industrial robots is important for improving the performance of the robots, in this paper, a simulation-based reliability design optimization method is proposed to improve the reliability of robots. Four steps including LHS, approximating the performance function based on simulation, establishing the reliability design optimization model and optimization solution based on the SORA algorithm were involved in the proposed method. The effectiveness of the proposed method was verified by the design of the big arm and the small arm of an industrial robot with a load of 6 Kg. Compared with the deterministic design optimization, the proposed method appeared to be more efficient in ensuring performance reliability. The verification results showed that the proposed method can successfully realize the reliability design of industrial robots. The verification results also demonstrated that the proposed method has a better computational efficiency compared with the reliability design optimization of the double-loop method.

In this paper, the reliability design optimization of the big arm and small arm of an industrial robot was performed under conditions which did not consider the dynamic performance and the design optimization of other connecting parts, and therefore a whole reliability design optimization method can be developed on the basis of the proposed method in the future. The influence of the jump resonance on the reliability of the robotic arms was also not considered in this research. In addition, the study considered a single-disciplinary reliability design optimization. However, the structural design of industrial robots is a problem involving multiple disciplines such as mechanical and electrical system and control. Consequently, the development of a multidisciplinary reliability design optimization method simultaneously considering static performance, dynamic performance and jump resonance will be the focus of future work, so as to further improve the performance of the industrial robot.

**Author Contributions:** Conceptualization, L.-X.Z. and X.-J.M.; methodology, L.-X.Z. and X.-J.M.; software, Z.-J.D. and H.-X.H.; validation, L.-X.Z., Z.-J.D. and H.-X.H.; formal analysis, X.-J.M.; investigation, Z.-J.D. and X.-J.M.; resources, X.-J.M.; data curation, L.-X.Z., Z.-J.D. and H.-X.H.; writing—original draft preparation, L.-X.Z. and Z.-J.D.; writing—review and editing, L.-X.Z. and X.-J.M.; visualization, L.-X.Z., X.-J.M. and Z.-J.D.; supervision, X.-J.M.; project administration, X.-J.M.; funding acquisition, X.-J.M. All authors have read and agreed to the published version of the manuscript.

**Funding:** This research was funded by the Natural Science Foundation of Hebei Province of China, grant number E2021402052, and the Science & Technology Research Program of Handan City of China, grant number 21422021299.

**Institutional Review Board Statement:** Not applicable.

**Informed Consent Statement:** Not applicable.

**Data Availability Statement:** The data are contained within the article.

**Conflicts of Interest:** The authors declare no conflict of interest.

## References


1. Arents, J.; Cacurs, R.; Greitans, M. Integration of computervision and artificial intelligence subsystems with robot operating system based motion planning for industrial robots. *Autom. Control Comput. Sci.* **2018**, *52*, 392–401. [CrossRef]
2. Gupta, V.; Saha, S.K.; Chaudhary, H. Optimum design of serial robots. *J. Mech. Des.* **2019**, *141*, 082303. [CrossRef]
3. Jamwal, A.; Agrawal, R.; Sharma, M.; Giallanza, A. Industry 4.0 technologies for manufacturing sustainability: A systematic review and future research directions. *Appl. Sci.* **2021**, *11*, 5725. [CrossRef]
4. Gerrikagoitia, J.K.; Unamuno, G.; Urkia, E.; Serna, A. Digital manufacturing platforms in the industry 4.0 from private and public perspectives. *Appl. Sci.* **2019**, *9*, 2934. [CrossRef]
5. Papakostas, N.; Constantinescu, C.; Mourtzis, D. Novel industry 4.0 technologies and applications. *Appl. Sci.* **2019**, *10*, 6498. [CrossRef]
6. Hsiao, J.C.; Shivam, K.; Chou, C.L.; Kam, T.Y. Shape design optimization of a robot arm using a surrogate-based evolutionary approach. *Appl. Sci.* **2020**, *10*, 2223. [CrossRef]
7. Kouritem, S.A.; Abouheaf, M.I.; Abouheaf, C.A.; Nahas, N.; Hassan, M. A multi-objective optimization design of industrial robot arms. *Alex. Eng. J.* **2022**, *61*, 12847–12867. [CrossRef]
8. Liang, M.X.; Li, Z.G.; Tang, R.Z.; Chen, L.; Huang, C. Structure optimization design of robot arm based on flexible multi-body dynamics. *China Mech. Eng.* **2017**, *28*, 2562–2566.
9. Bugday, M.; Karali, M. Design optimization of industrial robot arm to minimize redundant weight. *Eng. Sci. Technol. Int. J.* **2019**, *22*, 346–352. [CrossRef]
10. Mefteh, W. Simulation-based design: Overview about related works. *Math. Comput. Simul.* **2018**, *152*, 81–97. [CrossRef]
11. Ramasubramanian, A.K.; Connolly, M.; Mathew, R.; Papakostas, N. Automatic simulation-based design and validation of robotic gripper. *CIRP Ann.–Manuf. Technol.* **2022**, *71*, 137–140. [CrossRef]
12. Brathikan, V.M.; Prashanth, P.; Vikash, S.; Shri, M.V. Design and development of 5-axis robot. *Mater. Today Proc.* **2022**, *62*, 2179–2184.
13. Sahu, S.; Choudhury, B.B.; Biswal, B.B. A vibration analysis of a 6 axis industrial robot using FEA. *Mater. Today Proc.* **2017**, *4*, 2403–2410. [CrossRef]
14. Sahu, S.; Choudhury, B.B. Stress and modal analysis of six-axis articulated robot using ANSYS. *Inf. Commun. Technol. Compet. Strateg.* **2019**, *40*, 303–311.
15. Ghosh, A.; Roy, A.; Mishra, R.; Kamlesh, S.S. Structural optimization of a CT guided robotic arm based on static analysis. *Mater. Today Proc.* **2018**, *5*, 19586–19593. [CrossRef]
16. Shanmugasundar, G.; Sivaramakrishnanb, R.; Meganathanc, S.; Balasubramanid, S. Structural optimization of an Five Degrees of Freedom (T-3R-T) robot manipultor using finite element analysis. *Mater. Today Proc.* **2019**, *16*, 1325–1332. [CrossRef]
17. Shi, Y.; Lu, Z.Z.; Zhang, K.C.; Wei, Y.H. Reliability analysis for structures with multiple temporal and spatial parameters based on the effective first-crossing point. *J. Mech. Des.* **2017**, *139*, 121403. [CrossRef]
18. Salehghaffari, S.; Rais-Rohani, M. Material model uncertainty quantification using evidence theory. *Proc. Inst. Mech. Eng. Part C J. Mech. Eng. Sci.* **2013**, *227*, 2165–2181. [CrossRef]
19. Choi, C.K.; Yoo, H.H. Stochastic inverse method to identify parameter random fields in a structure. *Struct. Multidiscip. Optim.* **2016**, *54*, 1557–1571. [CrossRef]
20. Xu, X.; Chen, X.; Liu, Z.; Xu, Y.; Li, Y.; Gao, Y. *Dynamic-Static Optimization Design with Uncertain Parameters for Lift Arm of Parking Robot*; SAE Technical Papers: Warrendale, PA, USA, 2020; No. 2020-01-0511.
21. Wang, L.; Zhou, Z.; Liu, J. Interval-based optimal trajectory tracking control method for manipulators with clearance considering time-dependent reliability constraints. *Aerosp. Sci. Technol.* **2022**, *128*, 107745. [CrossRef]
22. Gao, Y.; Zhang, F.; Li, Y. Reliability optimization design of a planar multi-body system with two clearance joints based on reliability sensitivity analysis. *Proc. Inst. Mech. Eng. Part C J. Mech. Eng. Sci.* **2019**, *233*, 1369–1382. [CrossRef]
23. Lara-Molina, F.A.; Gonçalves, R.S. Reliability-based optimization of flexible manipulators. *J. Vib. Eng. Technol.* **2022**, 1–16. [CrossRef]
24. Lara-Molina, F.A.; Dumur, D. Robust multi-objective optimization of parallel manipulators. *Meccanica* **2021**, *56*, 2843–2860. [CrossRef]
25. Miroslav, V. Hierarchical refinement of Latin Hypercube Samples. *Comput. -Aided Civ. Infrastruct. Eng.* **2015**, *30*, 394–411.
26. Zhang, L.X.; Meng, X.J.; Zhang, H. Reliability-based design optimization for design problems with random fuzzy and interval uncertainties. *Int. J. Comput. Methods* **2020**, *17*, 1950018. [CrossRef]
27. Du, X.; Chen, W. Sequential optimization and reliability assessment method for efficient probabilistic design. *J. Mech. Des.* **2004**, *126*, 225–233. [CrossRef]

28. Meng, X.J.; Zhang, L.X.; Pan, Y.; Liu, Z.M. Reliability-based multidisciplinary concurrent design optimization method for complex engineering systems. *Eng. Optim.* **2022**, *54*, 1374–1394. [CrossRef]
29. Buscarino, A.; Famoso, C.; Fortuna, L.; Frasca, M. Multi-jump resonance systems. *Int. J. Control* **2020**, *93*, 282–292. [CrossRef]

**Disclaimer/Publisher's Note:** The statements, opinions and data contained in all publications are solely those of the individual author(s) and contributor(s) and not of MDPI and/or the editor(s). MDPI and/or the editor(s) disclaim responsibility for any injury to people or property resulting from any ideas, methods, instructions or products referred to in the content.